Mechanical and microstructure characterization of hard nanostructured N-bearing thin coating

M. Cabibbo, N. Clemente, M. El Mehtedi, S. Spigarelli, M. Daurù, A. S. Hammuda, F. Musharavati

Tools for machining are made of hard steels and cemented carbide (WC-Co). For specialized applications, such as aluminium machining, diamond or polycrystalline cubic boron nitride are also used. The main problem with steel, is that it exhibits a relatively low hardness (below 10GPa) which strongly decreases upon annealing above about 600K. Thus, the majority of modern tools are nowadays coated with hard coatings that increase the hardness, decrease the coefficient of friction and protect the tools against oxidation. A similar approach has been recently used to obtain a longer duration of the dies for aluminium die-casting. Multi-component and nanostructured materials represent a promising class of protective hard coatings due to their enhanced mechanical and thermal oxidation properties. Surface properties modification is an effective way to improve the performances of materials subjected to thermo-mechanical stress. Three different thin hard nitrogen-rich coatings were mechanically, microstructurally, and thermally characterized: a 2.5 micron-thick CrN-NbN, a 11.7 micron-thick TiAlN, and a 2.92 micron-thick AlTiCrxNy. The CrN-NbN coating main feature is the fabrication by the alternate deposition of 4nm thick-nanolayer of NewChrome (new type of CrN, with strong adhesion and low coating temperature). All the three coatings can reach hardness and elastic modulus in excess of 20, and 250 GPa, respectively. Their main applications include stainless steel drawing, plastic materials forming and extrusion and aluminum alloys die-casting. The here studied TiAlN (SBN, super booster nitride) is one of the latest evolution of TiAlN coatings for cutting applications, where maximum resistance to wear and oxidation are required. The AlTiCrxNy combines the very high wear resistance characteristic of the Cr-coatings and the high thermal stability and high-temperature hardness typical of Al-containing coatings.
All the coatings were deposited on a S600 tool steels. The coatings were subjected to two different thermal cycling tests: one for 100 thermal cycles consisting of 60 s dwelling time, respectively at the high- (573 to 1173 K) and at the room-temperature, a second for 100 thermal cycles consisting of 115s dwelling time, at same temperatures of the first test, followed by 5s dwelling at room-temperature. The investigated coatings showed a sufficient-to-optimal thermal response in terms of stability of hardness, elastic modulus, and oxidation behavior. The temperature induced hardness and elastic modulus coating variations were measured by nanoindentation.

Keywords: Nanostructured coatings - Thermal cycling - Nanoindentation - FEGSEM

Marcello Cabibbo, Nicola Clemente, Mohamad El Mehtedi, Stefano Spigarelli
Dipartimento di Ingegneria Industriale e Scienze Matematiche (DIISM), Università Politecnica delle Marche, I-60131, Ancona – Italia.
Mauro Daurù
Lafer SpA, Strada di Cortemaggiore 31 29122 Piacenza, Italy.
Abdelmagid S. Hammuda, Farayi Musharavati
Department of Mechanical and Industrial Engineering, Qatar University, Doha, Qatar

Corresponding author:
Marcello Cabibbo, e-mail: m.cabibbo@univpm.it
Phone: +39 0712204728: Fax: +390712204770

INTRODUCTION

Hard coatings are increasingly required for wear resistant applications on tools, dies, molds, and for components used in the automotive and aerospace industries, which always are exposed to severe tribological and thermal conditions.
Environmental pressures, however, have initiated a worldwide research for its replacement. Among the different valuable substitutes, chromium nitride films, with their good oxidation, anticorrosive and anti-adhesive properties, find a wide industrial use in metal forming and plastic molding operations [1]. The low hardness and abrasive wear resistance of CrN are the main reasons, why CrN has not used successfully in steel cutting applications [1].
In fact, nitride based hard compound coatings prepared by various physical vapor deposition processes are found increasing applications for nearly every demand. High hardness, excellent wear and corrosion resistance enable

	Chemical composition	Type of the structures	Type of Deposition	Thickness [μm]	Surface Roughness [mm]
SLC	$Cr_{0.336}Nb_{0.182}N_{0.482}$	nano-layered	evaporation arc - PVD	2.61	0.12
ALOX	$Ti_{0.5}Al_{0.5}N$	mono-layered	magnetron sputtering	11.71	0.07
TIGRAL	$AlTiCr_xN_{1-x}$	multi-layered	Cr/Ti-Al - PVD	2.92	0.10

Tab. 1 - Composition and characteristics of the three coatings produced by Lafer® and tested in this study (as-deposited conditions).

them to improve tool life greatly [2]. Among them, TiN and CrN are respectively the first and the second most frequently employed coatings. Various alloying elements have been added to improve the properties of the coatings. The addition of aluminum to form ternary thin films, e.g. TiAlN and CrAlN are particularly attractive. Some studies have conformed their excellent oxidation resistance [3], good mechanical properties [4], and suitable application as cutting tools [5].

On this basis, due to the advanced tribology properties and to the high temperature oxidation resistance, industrial applications of the single and multi-layer TiAlN coatings, synthesized by physical vapor deposition (PVD), are increasing rapidly [6]. On the other hand, the incorporation of Al in the cubic fcc TiN matrix leads to a noticeable enhanced coating thermal stability [7].

Theoretically, multilayer coatings are expected to have higher cracking resistance than monolithic coatings due to differences in material constants within constituent layers. In fact, multilayered coatings have shown enhanced mechanical and tribological properties compared to single layers of TiN, TiCN and (Ti,Al)N [8,9]. These multilayered films of micrometer-to-nanometer level periodicity (with the same total thickness as single layer coatings) are deposited by alternating two different materials from separate sources, and are generally deposited on a nanometer range.

The main disadvantage of TiN is its limited oxidation resistance (approximately 600–700K). The addition of other elements, such as Al, Cr, Si, and others, are likely to increase the oxidation resistance of TiN [10]. In the attempt of adding Cr, research shows that a slight addition of Cr to AlTiN results in excellent cutting performance [11]. The thermodynamically metastable, ternary-phase$Ti_{1-x}Al_xN$ shows high micro-hardness, high oxidation stability, low coefficient of thermal conduction and lowfriction against steel substrates. Because of all these remarkable advantages $Ti_{1-x}Al_xN$ coatings are successfully applied today for dry cutting operations and high-speed machining of cast iron and die steels [12]. It is reported that the hardness and oxidation resistance of $(Ti_{1-x}Al_x)N$ coating can be increased as the Al ratio x increased up to approximately 0.6–0.7. However, further addition of Al yields a formation of soft hexagonal phase in the coating and results in significant loss of mechanical property (the around Al ratio being of 0.4-to-0.67 for the phase transformation from cubic to hexagonal) [13].

NbN-based coatings have been studied on various steel substrates, such mild steel, stainless steel, and high speed steel (HSS). Different deposition techniques were used, among these the reactive DC magnetron sputtering, at various nitrogen flow rates, and substrate biasing is able to guarantee coating soundness and high mechanical properties.

This work presents results on thermal stability of three superhard coatings on tool steel. CrNbN, TiAlN, and a AlTiCrN coatings were tested under thermal cycling up to temperatures of 1173K. Mechanical and microstructure characterization was carried out using nanoindentation and electron microscopy techniques, respectively.

EXPERIMENTAL PROCEDURES

The coatings. Three coatings were deposited on S600 HSS steel flat samples hardened to 61 - 63 HRC and lapped to Ra<0,04 mm and. All the coating were deposited by Lafer© and their chemical and morphological characteristics are reported in the Table 1.

Thermal cycles. To test and verify the soundness and the oxidation behavior of all the coatings, thermal cycling tests at different temperatures were carried out. These tests were performed for temperatures of 1073, 1173, and 1273K. All the coated steels were subjected to two types of thermal tests for a total of 100 cycles. The first test was conducted with each cycle consisted of 60s of baking at the set temperature, followed by a room temperature (RT) quenching and maintenance at RT for 60s. The second test was conducted with each cycle consisting of 115s dwelling at the set temperature, RT quenching and 5s at RT. In both the cases, the heating rate was 5K/min to 900K, followed by 3K/min up to the set temperature.

FEGSEM inspections. Cross sections of the coating-substrate polished samples were inspected with a high resolution scanning electron microscope (FEG-SEM) Zeiss™ Supra® 40. To visually distinguish the coating thickness extension from the steel substrate, the backscattered electrons (BSE) signal was used. In order to make the signal as bright and well-contrasted as possible, observations were performed using a high accelerating voltage of 15kV. The exact measurements of the coating thickness versus

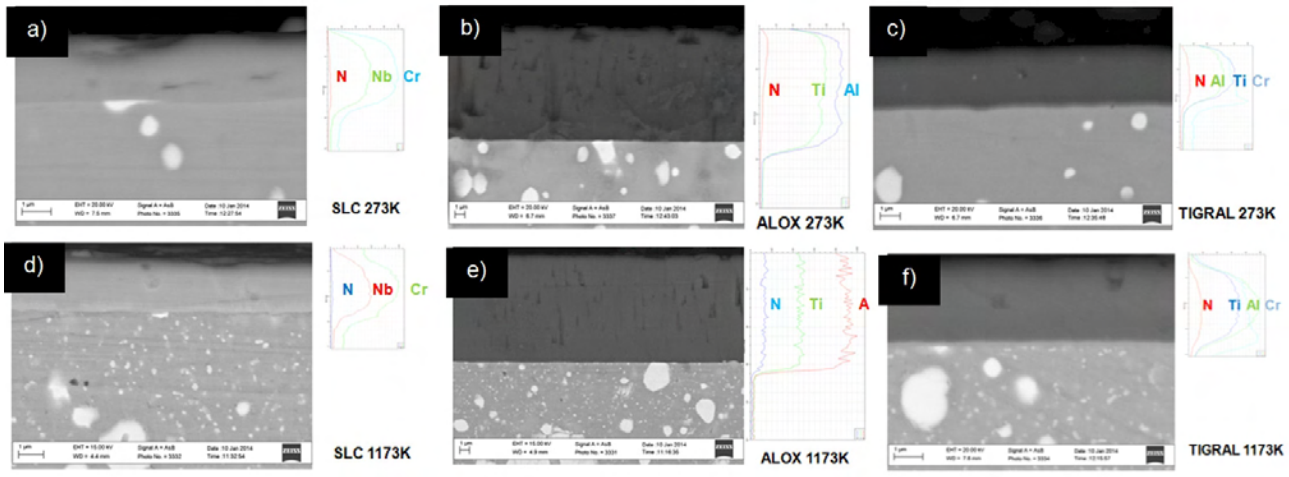

Fig. 1 - FEGSEM BS (Back Scattered) images, with superimposed EDS profiles, of the SLC, ALOX, and TIGRAL. As-deposited conditions: a), b), and c); after thermal cycling at 1173 K: d), e), and f).

the different thermal cycling conditions, was carried out using EDS (energy-dispersive signal) of N, for all the three coatings, of Cr and Nb; Ti and Al; Ti, Al and Cr, for the SLC, ALOX, and TIGRAL, respectively.

Nanoindentation and Roughness tests. A UBI-1® Hysitron-™ Triboscan nanoindenter, equipped with triangular Berkovich tip was used. Tip calibration was carried out using the standard procedure. The maximum load was fixed at 10mN. A trapezoidal load function (30s load to the maximum load value, maintenance for 10s, and unloading in 30s) was used. To obtain statistically reliable data, for each experimental condition, matrix of 8x8 (64) indents were carried out.

The nanoindentation measurements were analyzed using the Oliver and Pharr method [14,15]. Therefore, hardness and reduced Young's modulus are obtained after a complete cycle of load-unloading cycle of the indenter. The unloading curve is fitted with a power-law relationship (Eq. 1):

$$P = B(h-h_f)^m \qquad (1)$$

where P is the tip load, h the displacement, h_f is the displacement after unloading, B and m are fitting parameters. The contact depth, h_c, can be estimated from the load-displacement data as (Eq. 2):

$$h_c = h_{max} - \varepsilon(P_{max}/S) \qquad (2)$$

where h_{max} is the maximum indenter penetration depth at the peak load, P_{max}, e is a tip dependent constant, S, is the material stiffness. For a Berkovich tip, e = 0.75 [15,16].

Calibration was carried out on fused quartz (E_r = 72GPa), according to the specifications and recommendation resulting from a round robin experiment recently published by two of the present authors [16] (to which the reader is addressed for further details).

Roughness. Roughness was measured by Mitutoyo™ SJ-301 roughness-meter along 6 different paths for each experimental condition. Mean roughness, R_a, was obtained by taking in account the 6 different measurements.

Results and discussion

In order to better correlate the morphological integrity of the three coatings, roughness measurements and coating thickness, by electron microscopy, were carried out. The coatings surface roughness, after the different thermal cycling temperatures, is reported in the Table 2. It is was found that in all the three coatings, and for the whole range of thermal cycling temperatures (1073, 1173, and 1273K) no significant roughness modification occurred.

The FEGSEM inspections of Fig. 1 focused on the exact coating measurement through the EDS line analysis of the chemical elements of which the coatings were made, that is: N, Cr, and Nb, for the SLC; N, Ti, and Al, for the ALOX; N, Al, Ti, and Cr, for the TIGRAL. Figure 1 reports the FEGSEM BS images, with superimposed the EDS signals, for the three coatings in the as-deposited condition, and after the maximum thermal cycling temperature (1273K). The ALOX and the TIGRAL coatings did not reduce their thickness under the thermal cycling exposure. Yet, the SLC showed a significant thickness reduction, which more than halved at 1273K.

It is worth to note that a fraction of the heavy metals of which the coatings are made, diffused into the substrate steel. Thus, some of the Nb, and Cr diffused into the HSS steel from the SLC coating, at 1273K. Some of the Ti, and a greater part of Al, diffused into the steel from the ALOX coating. Ti, Al, and Cr diffused from the TIGRAL into the beneath steel at 1273K. The reduced coating thickness observed in the case of the SLC is likely to contribute to the Hardness reduction, respect to the as-deposited condition, recorded starting from 1073K.

The roughness variation (Table 2), recorded at all the experimental condition, did not show any significant modification with respect to the as-deposited condition.

Mechanical Response. Representative load-unload curves for all the three coatings and substrates are reported in the Figure 2. In the 60s in / 60s out thermal cycle, although the penetration depth span over few tens of nanometers, the load-displacement curves show quite a narrow unload slope range. This holds especially in the case of the

Thermal cycle	Coating	Roughness, [μm]	as-dep.	1073K	1173K	1273K
60 s in / 60 s out	SLC	Ra	0.12 ± 0.01	0.09 ± 0.01	0.11 ± 0.01	0.11 ± 0.01
	ALOX	Ra	0.07 ± 0.01	0.10 ± 0.01	0.13 ± 0.01	0.14 ± 0.01
	TIGRAL	Ra	0.10 ± 0.01	0.10 ± 0.01	0.11 ± 0.01	0.11 ± 0.01
115 s in / 5 s out	SLC	Ra	0.12 ± 0.01	0.12 ± 0.01	0.13 ± 0.01	0.12 ± 0.01
	ALOX	Ra	0.07 ± 0.01	0.09 ± 0.01	0.13 ± 0.01	0.13 ± 0.01
	TIGRAL	Ra	0.10 ± 0.01	0.12 ± 0.01	0.11 ± 0.01	0.13 ± 0.01

Tab. 2 - Mean Roughness, R_a, of the three coatings at the three thermal cycling temperatures of 1073, 1173, 1273

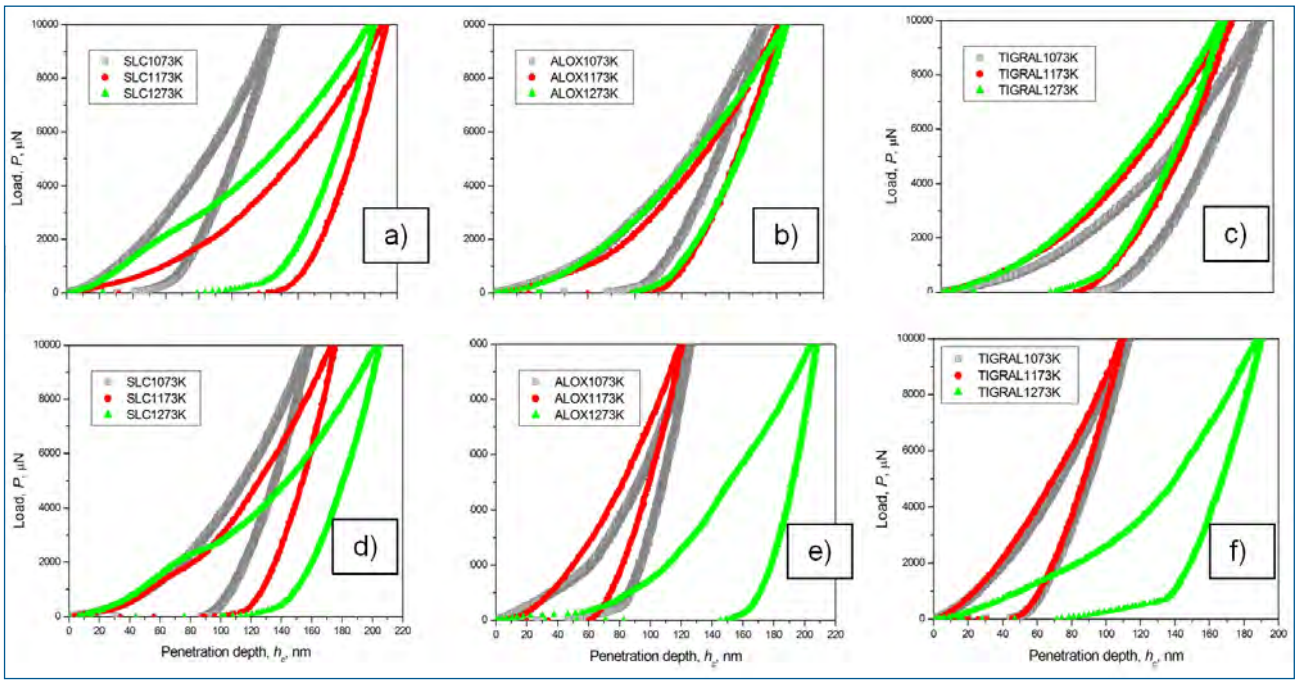

Fig. 2 - Representative load-displacement nanoindentation curves of SLC, ALOX, and TIGRAL coatings for thermal cycling temperatures 1073, 1173, and 1273K, in both configurations: cycles of 60s in and 60s out, a), b), and c); and cycles of 115s in and 5s out, d), e), and f).

ALOX and TIGRAL coatings. That is, the nanoindentation measurements showed quite a similar mechanical response, either in terms of hardness and elastic modulus, over most of the thermal cycling temperatures to which the three different HSS S-600/coating systems were subjected. This is not longer the case for the 115s in / 5s out thermal cycle, for the ALOX and TIGRAL coatings, where at the highest temperature to which the three coatings were subjected (1273K), showed a considerably larger penetration depth, respect to the lower cycling temperatures.

Table 3 shows the hardness, *H*, and the reduced elastic modulus, E_r, in terms of the thermal cycling temperatures and cycle type. In the 60s in/60s out thermal cycle, the SLC coating hardness almost halved from 1073 K to 1273K. On the other hand, the two Al-Ti-N-bearing coatings (ALOX and TIGRAL) retained their hardness of 20-22GPa up to the maximum thermal cycling temperature of 1273K. At the same time, the coating elastic modulus did not show any significant reduction with the cycling temperatures. It is worth to note that the two Al-Ti-N coatings (ALOX and TIGRAL) have a higher elastic modulus (which accounted for 30-40% larger values) with respect to Cr-Nb-N (SLC) coating. In the second thermal cycle of 115s in / 5s out, the SLC coating hardness reduced to a larger extent, from 1073 K to 1273K, with respect the first thermal cycle. In this second thermal cycle, the ALOX and TIGRAL coatings maintained their hardness up to 1173K to yield and reduce to more than 50% at 1273K. The elastic modulus of the three coatings did not show any significant reduction with the cycling temperatures, and again, the two Al-Ti-N coatings (ALOX and TIGRAL) had a higher elastic modulus (which still accounted for 30-40% larger values) with respect to Cr-Nb-N (SLC) coating.

CONCLUSIONS

At 1173K the $Cr_{0.336}Nb_{0.182}N_{0.482}$ nano-layered (SLC) coating showed oxidation phenomena and a hardness drastic reduction to half of the as-deposited value, while the elastic

Thermal cycle	Mechanical property	Coating	as-dep.	1073K	1173K	1273K
60 s in / 60 s out	H	SLC	22 ± 0.01	20 ± 0.01	11 ± 1	12 ± 1
		ALOX	23 ± 0.01	22 ± 0.01	20 ± 2	20 ± 3
		TIGRAL	24 ± 0.01	22 ± 0.01	22 ± 2	22 ± 2
	E	SLC	270 ± 10	290 ± 30	250 ± 30	230 ± 20
		ALOX	450 ± 10	350 ± 0.01	370 ± 40	380 ± 50
		TIGRAL	300 ± 10	330 ± 0.01	350 ± 40	330 ± 20
115 s in / 5 s out	H	SLC	22 ± 1	16 ± 2	11 ± 2	9 ± 1
		ALOX	23 ± 1	21 ± 2	21 ± 2	8 ± 2
		TIGRAL	24 ± 1	22 ± 2	22 ± 1	11 ± 2
	E	SLC	270 ± 10	260 ± 20	250 ± 30	210 ± 20
		ALOX	450 ± 10	360 ± 50	370 ± 50	300 ± 60
		TIGRAL	300 ± 10	330 ± 20	340 ± 30	240 ± 20

Tab. 3 - Mean Roughness, R_a, of the three coatings at the three thermal cycling temperatures of 1073, 1173, 1273 K, for the two types of cycle.

modulus remained unchanged up to 1273 K.
The unique advantage of the AlTiCr$_x$N$_{1-x}$ multilayer (TIGRAL) coatings is their exceptional properties, such as: very high oxidation resistance (up to 1273 K) with stable high hardness of 20–22 GPa. These hardness values are retained up to 1273K, in the less drastic 100-thermal cycle test, and up to 1173 K, under 100 thermal cycling exposure either in the less drastic condition of 60s in and 60s out, and in the more drastic condition of 115s in and 5s out. Roughness remained virtually unchanged at all the tested temperatures (1073, 1173, and 1273 K), revealing a substantially fair thermodynamic stability of the coatings.
The very thin alumina oxide film that form during thermal exposure is likely to guarantee high wear resistance during high-speed machining of the cutting tool surface, as the most important mechanical properties for this kind of applications is the coating hardness and its adhesion strength to the metallic substrate.

ACKNOWLEDGMENTS

This publication was made possible by NPRP grant # NPRP 5-423-2-167, entitled: *"Advanced ultra-hard Nanostructured Coatings for innovative applications in mechanical and chemical industries"*, from the Qatar National Research Fund (a member of Qatar Foundation). The statements made herein are solely the responsibility of the authors.

RIFERIMENTI BIBLIOGRAFICI

1] J. VETTER, Surf. Coat. Technol. 76 (1995) 719.
2] K. SINGH, P.-K. LIMAYE, N.L. SONI, A.K. GROVER, R.G. AGRAWAL, A.K. SURI, Wear 258 (2005) 1813.
3] M. KAWATE, A.K. HASHIMOTO, T. SUZUKI, Surf. Coat. Technol. 165 (2003) 163.
4] H.C. BARSHILIA, M.S. PRAKASH, A. JAIN, K.S. RAJAM, Vacuum 77 (2005) 169.
5] C. NOUVEAU, C. LABIDI, J.-F. FERREIRA MARTIN, R. COLLET, A. DJOUADI, Wear 263 (2007) 1291.
6] S.G. HARRIS, E.D. DOYLE, A.C. VLASVELD, J. AUDY, D. QUICK, Wear 254 (2003) 723.
7] F. WEBER, F. FONTAINE, M. SCHEIB, W. BOCK, Surf. Coat. Technol. 177–178 (2004) 227.
8] M. NORDIN, M. LARSSON, S. HOGMARK, Surf. Coat. Technol. 106 (1998) 234.
9] P.C. YASHAR, W.D. SPROUL, Vacuum 55 (1999) 179.
10] F. VAZ, L. REBOUTA, M. ANDRITSCHKY, M.F. DA SILVA, J.C. SOARES, J. Mater. Process. Technol. 92–93 (1999) 169.
11] G.S. FOX-RABINOVICH, K. YAMAMOTO, S.C. VELDHUIS, A.I. KOVALEV, G K. DOSBAEVA, Surf. Coat. Technol. 200 (2005) 1804.
12] S. VEPREK, J. Vac. Sci. Technol. A 17 (1999) 2401.
13] U. WAHLSTROM, L. HULTMAN, J.-E. SUNDGREN, I. PERTOV, F. ADIBI, J.E. GREENE, Thin Solid Films 235 (1991) 62.
14] G M. PHARR, Mater. Sci. Eng. A, 253 (1998) 151.
15] M. F. DOERNER, W.D. NIX, J. Mater. Res. 1 (1986) 601.
16] M. CABIBBO, P. RICCI, R. CECCHINI, Z. RYMUZA, J. SULLIVAN, S. DUB, S. COHEN, Micron 43 (2012) 215.
17] J.L. MO, M.H. ZHU, A. LEYLAND, A. MATTHEWS, Surf. Coat. Technol. 215 (2013) 170.
18] Y.-J. LIN, A. AGRAWAL, Y. FANG, Wear 264 (2008) 226.
19] Y.-Y. CHANG, D.-Y. WANG, Surf. Coat. Technol. 201 (2007) 6699.
20] D. JAKUBECZYOVA, P. HVIZDOS, M. SELECKA, App. Surf. Sci. 258 (2012) 5105.